INSTITUTE OF PHYSICS PUBLISHING JOURNAL OF PHYSICS B: ATOMIC, MOLECULAR AND OPTICAL PHYSICS

J. Phys. B: At. Mol. Opt. Phys. **37** (2004) L321–L328 PII: S0953-4075(04)81097-6

LETTER TO THE EDITOR

Multi-electron emission from fullerenes upon a single photon absorption

O Kidun[1], **N Fominykh**[2] **and J Berakdar**[1]

[1] Max-Planck Institut für Mikrostruktur Physik, Weinberg 2, 06120 Halle, Germany
[2] Institute of Physics, Ulyanovskaya 1, St Petersburg, 198904, Russia

Received 20 May 2004
Published 24 August 2004
Online at stacks.iop.org/JPhysB/37/L321
doi:10.1088/0953-4075/37/17/L03

Abstract

A theoretical model is developed for the treatment of single and coincident multi-electron emission from a C_{60} molecule following the absorption of a VUV photon. The multi-electron ionization process is viewed as a single electron–photon interaction followed by a sequence of incoherent electron–electron collisions in which the photon energy is distributed among the emitted electrons. The single-particle states of C_{60} are calculated within the Hartree–Fock and the spherical jellium approximation whereas many-body effects are treated on the basis of the random-phase approximation with exchange. Quantum mechanical transition amplitudes and cross sections are evaluated numerically and compared with available experiments.

(Some figures in this article are in colour only in the electronic version)

1. Introduction

Carbon fullerene molecules, such as C_{60}, offer an opportunity to investigate the crossover between atomic and condensed matter behaviour. On the one hand, C_{60} contains a relatively small number of ionic sites (60 carbon atoms), but on the other the atomic sites are ordered (which results in diffraction-like phenomena). The valence shell contains a relatively large number of delocalized electrons which renders possible effects akin to condensed matter systems, such as dielectric screening [1] and the onset of plasmon formation [2]. In addition to these attractive features for fundamental research fullerenes turned out to be a promising candidate for application in nano and molecular electronic devices [3, 4]. The remarkable symmetry of the buckyball structure of the fullerenes makes these molecules exceptionally stable. This is manifested in the experimental facts that various important physical and chemical properties of isolated fullerene molecules persist in the solid phase [5–7]. Thus, it is of general significance to study the properties of the gas-phase C_{60}. Phenomena of particular interest for this work are those driven by the correlation between the valence electrons. Due to

the unsaturated character of the C–C bonds of the fullerene a considerable number of valence electronic states (240 e^- for C_{60}) are delocalized over the molecular surface. These states take part in various electronic excitations [2] that are induced by external perturbations, such as excitations and ionization by the impact of photons or charged particles. The process of the photon and electron-impact ionization of a many-particle system is a useful and in some aspects a unique tool for studying the correlated electron dynamics. For example, processes such as the simultaneous emission of two or more electrons in response to the absorption of a single photon cannot be realistically modelled within an independent electron approximation. Therefore, the analysis of the multiple ionization spectra offers a new insight into the details of the correlated electron motion in nanosize systems. The information obtained thus is complementary to the outcome of spectroscopic methods where the number of particles in the target is not changed, such as electron-energy loss spectroscopy (EELS) (which tests for the density–density correlation) and photoabsorption spectroscopy [8, 9]. Currently experimental data exist for the C_{60} single ionization cross sections following the impact of photons [10, 11] and charged particle impact [12–14]. Recently, the first experiment for the one-photon double ionization of C_{60} was conducted [15, 16]. In view of this development it is timely to consider the theoretical aspects of the one-photon multiple ionization of C_{60}, which is done in this work. We aim at calculating the C_{60} single and multiple photoionization cross sections within the same model, to allow for a sensible estimation of the ratios between the magnitudes of the various n-fold ionization events.

2. Incoherent multiple photoionization

The term multiple photoionization (MPI) is used for the process in which, after the absorption of a *single* (VUV) photon, two or more electrons escape to the continuum leaving the fullerene in the stable two-fold or higher ionized state. Upon absorption of the photon the radiation energy is transferred to the electronic degrees of freedom of the target. This energy is partly spent on ionization (to overcome the binding energy of the electrons and to deliver a certain amount of kinetic energy). Some part of the deposited energy is transferred to the vibrational degrees of freedom, i.e. to the internal energy of the molecular ion. The subsequent dissociation of the excited molecular ion may be accompanied by the emission of photons, delayed electrons emission or small fragments formation. In addition to the direct knock-out of electrons, other processes such as shake-off, Auger decay, multiple excitations may contribute significantly. This complexity of the problem makes a theoretical treatment of all the facets of MPI a challenging task. In fact, to the best of our knowledge there is no theoretical description of the MPI processes of fullerenes available yet. To develop such a theory we operate within the dipole approximation for the photon field[3]. The differential cross section of the n-fold ionization in the length form reads

$$\frac{\mathrm{d}^{3n}\sigma_n}{\mathrm{d}\mathbf{k}_1\cdots\mathrm{d}\mathbf{k}_n} = 4\pi^2\alpha\omega|T_n(\omega;\phi_1,\ldots,\phi_n;\mathbf{k}_1,\ldots,\mathbf{k}_n)|^2\delta\left(\omega+\epsilon_n-\sum_{i=1}^{n}E_i\right). \tag{1}$$

The n-particle mean-square transition amplitude $|T_n|^2$ depends on the initial one-electron states ϕ_i of the fullerene as well as on the states of the photoelectrons with the asymptotic wave vectors

[3] The photon-energy range for the validity of the dipole approximation in the case of fullerenes is significantly smaller than that for atoms. The dipole approximation relies on the magnitude of the incident electromagnetic field being (nearly) constant on the length scale of the system, $k_\omega D \ll 1$, where k_ω is the photon wave vector and $D \approx 13.3$ au is the 'size' of the target. For a photon energy E_ω the dispersion relation implies $E_\omega = \hbar\omega = \hbar k_\omega c$ (where $c \approx 137$ au is the light velocity and $\hbar = 1$ au). Thus we conclude that $D\omega/c = (13.3/137)\omega \ll 1$, meaning that $\omega \ll 10.3$ [Hartree] ≈ 280 [eV].

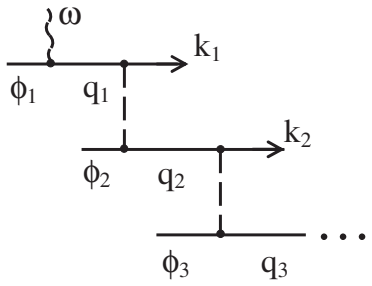

Figure 1. Schematic representation of the multiple photoionization process as calculated within our model: the single photoionization event is followed by $(n-1)$ electron–electron collisions, described in the RPAE approximation. Here ϕ, q, k denote the bound state, the intermediate state and the asymptotic wave vector of the scattering state, respectively.

$\mathbf{k}_i$ and energies E_i. $\alpha \approx 1/137$ is the fine structure constant. The n-fold ionization threshold is denoted by ϵ_n. The explicit form of T_n will be discussed now. Since the photon–C_{60} coupling is of a single-particle nature, the inter-electron interaction is ultimately responsible for the *multiple* electron emission. Specifically, a valence electron that absorbs the photon scatters from another valence electron (so-called (e, 2e) process). Both electrons are then elevated to vacuum states resulting thus in a double ionization event. In addition, one (or the other) of these high-energy electrons may scatter from a further valence electron leading thus to a triple ionization of C_{60}. Further, n-fold ($n > 3$) ionization events occur within this successive scattering scheme. From this scenario of multiple ionization it is comprehensible that the n-fold mean-square matrix element $|T_n|^2$ possesses a power law dependence on the mean-square Coulomb matrix element $|T_{\mathrm{e\,2e}}|^2$. The latter is a measure for the probability of a two-particle scattering. In addition, since the whole reaction is triggered by a single photoabsorption event, $|T_n|^2$ is linearly proportional to the mean square of the single photoionization transition amplitude $|T_\omega|^2$. The MPI probability P_n is therefore a product of probabilities of independent electron–photon and pairwise electron–electron collisions $P_n = P_\omega \cdot P_{\mathrm{e\,2e}}^{(1)} \cdot \ldots \cdot P_{\mathrm{e\,2e}}^{(n-1)}$, where the upper index denotes the ordering of successive (e, 2e)-events. More specifically, in terms of the single-particle states the n-fold mean-square matrix element $|T_n|^2$ is expressed as

$$\left|T_n\left(\omega;\phi_{\epsilon_1},\ldots,\phi_{\epsilon_n};\mathbf{k}_1,\ldots,\mathbf{k}_n\right)\right|^2 = \int\!\ldots\!\int \left|T_\omega\left(\omega,\phi_{\epsilon_1};\mathbf{q}_1\right)\right|^2 \cdot \delta\left(\omega+\epsilon_1-\frac{q_1^2}{2}\right) \times \prod_{i=1}^{n-1}\left|T_{\mathrm{e\,2e}}\left(\mathbf{q}_i,\phi_{\epsilon_{i+1}};\mathbf{q}_{i+1},\mathbf{k}_i\right)\right|^2 \delta\left(\frac{q_i^2}{2}+\epsilon_{i+1}-\frac{q_{i+1}^2}{2}-\frac{k_i^2}{2}\right)\mathrm{d}^3\,\mathbf{q}_i, \tag{2}$$

where ϵ_{i+1} is the binding energy of the target state $\phi_{\epsilon_{i+1}}$ and $\mathbf{q}_i$ is the wave vector of the intermediate (undetected) state, as illustrated in the diagram in figure 1. In this diagram energy conservation is implied at every vertex (exchange is implied and performed at the vertex).

Thus, the major ingredients for the calculations of $\mathrm{d}^{3n}\sigma$ are the single photoionization (SPI) matrix elements and the (e, 2e) transition amplitudes accompanied by an appropriate averaging over the intermediate states. It may appear that the present theory has a resemblance to the known statistical energy-deposition model [17] (or its variations) which has, for example, been recently applied to the ion-impact multiple ionization of atoms and fullerenes in [13] and by Hansen *et al* (cf [18] and references therein) for the description of fast multiple photon absorption during irradiation with a laser beam. In this context, we stress that our aim here is to

go beyond statistical approaches in order to incorporate (1) the quantal behaviour of the target electronic states, (2) the quantum aspects of electron–electron scattering photoionization and (3) the quantum many-body effects as a renormalization of the electron–electron vertex. These achievements come at the cost of using some simplifying approximations (e.g., Hartree–Fock, single scattering and random-phase approximation with exchange (RPAE)). In contrast, the electron wavefunctions and many-body effects are not considered by conventional statistical models and the Coulomb matrix elements are taken as a free adjustable parameter.

2.1. Single photoionization transitions

The absorption time of the photon is well below the characteristic time of the vibrational motion of the molecule. Thus, it is reasonable to assume that the photon transfers the energy to a fixed in space (ground-state) molecule. Furthermore, the emission process is viewed within the sudden approximation, meaning that ionization is unaffected by electronic relaxation processes following the electron emission (such processes are incorporated in our model only at the level of RPAE for $T_{\mathrm{e}\,2\mathrm{e}}$, i.e. as a linear response of the electronic charge density). The one-electron transition amplitude $T_\omega\big(\omega, \phi_{\epsilon_i}; \mathbf{q}_i\big)$ is calculated according to

$$T_\omega\big(\omega, \phi_{\epsilon_i}; \mathbf{q}_i\big) = \hat{\mathbf{e}} \cdot \big\langle \psi_{\mathbf{q}_i}(\mathbf{r}_i) \big| \mathbf{r}_i \big| \phi_{\epsilon_i}(\mathbf{r}_i) \big\rangle, \tag{3}$$

where $\hat{\mathbf{e}}$ is the polarization vector of the linear-polarized photon. $T_\omega\big(\omega, \phi_{\epsilon_i}; \mathbf{q}_i\big)$ describes the transition of the one-electron orbital $\phi_{\epsilon_i}(\mathbf{r}_i)$ with the energy $\epsilon_i < 0$ to the scattering state $\psi_{\mathbf{q}_i}(\mathbf{r}_i)$ characterized by the wave vector $\mathbf{q}_i$ with $q_i^2/2 = \omega + \epsilon_i$. The one-electron state calculations are performed within the Hartree–Fock (HF) model, i.e. we incorporate the mean-field part of electron–electron interaction and exchange effects. The bound and the scattering wavefunctions are evaluated using the nonlocal variable phase approach [19–21].

The large number of valence electrons of the fullerene molecule makes *ab initio* calculations even of the HF wavefunctions and of the energy levels a challenging numerical task. Thus, one has to resort to some approximative schemes for the ionic potentials experienced by the valence electrons. In this work, a model potential of a fullerene shell is used, as explained in [22] (and references therein). Three decisive parameters define the model potential. The values we use for these parameters have been determined experimentally. These parameters are: the radius of the fullerene $R = 6.65a_0$ (a_0 is the Bohr radius), the distance between neighbouring carbon nuclei (C–C bond length) $\delta = 2.69a_0$ and the first ionization potential of the molecule $I_1 = 7.6\,\mathrm{eV}$. The potential of C_{60}, formed by carbon ions and localized core electrons, is modelled by a shifted potential well: $V_{\mathrm{ion}}(r) = V_0$ within the interval $R - \delta < r < R$, and $V = 0$ elsewhere. The potential depth V_0 is chosen such as to yield the experimental value of the first ionization potential and to encompass 240 valence electrons. The one-electron potential then represents a sum of the ionic background $V_{\mathrm{ion}}(r)$ and a self-consistent electronic density of all valence electrons. Having calculated the single-particle orbitals, the matrix elements are evaluated according to equations (3) and (2). To obtain integrated cross sections, numerical integration (using a Monte Carlo procedure) is performed over the relevant variables. Figure 2 shows the total single photoionization cross section of the highest occupied molecular orbital (HOMO) and HOMO-1 as a function of the photon energy. The photocurrent is normalized to the number of electrons in the HOMO (and HOMO-1) of the real molecule having icosahedral symmetry (within our model the HOMO orbital momentum is $\ell_{\mathrm{HOMO}} = 8$). A notable feature which is discussed in the literature (see e.g. [10, 11, 23, 24]) is the scattering of the photoelectron waves from the well boundaries. In a simplified picture, if we suppress for a moment the Hartree–Fock corrections to the one-electron potential, the photoelectron wave emitted from the origin encounters on its way

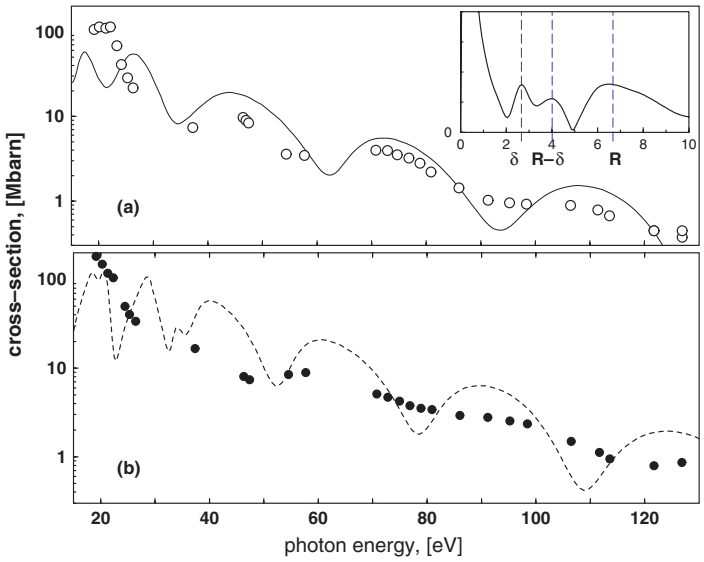

Figure 2. (a) The single photoionization cross section of the highest occupied molecular orbital (HOMO) of C_{60} versus photon energy, and (b) the same cross section for HOMO-1. Solid and dashed curves in (a) and (b) are present calculations. Open (a) and full (b) circles experimental data (taken from [10]). The photon polarization is linear. The orbital bound energy of HOMO is $\epsilon_{\mathrm{HOMO}} \sim -7.65$ eV. The inset in (a) shows the Fourier transform (FT) of the photoionization cross section $\sigma(k)$ from HOMO as a function of the photoelectron wave vector $k = \sqrt{2(\omega + \epsilon_{\mathrm{HOMO}})}$. The marked maxima in the FT correspond to the following characteristic lengths: fullerene shell radius R, C–C bond length δ and $R - \delta$.

to infinity two sharp potential edges. Consequently, the two characteristic lengths R and δ result in oscillations in the photoionization cross section (as a function of the photoelectron momentum) with two resonant frequencies (along with two nearest satellites). This statement is endorsed by Fourier-transforming the momentum-dependent photoionization cross section (inset figure 2) which possesses peaks located at the lengths δ, $R - \delta$, R and $R + \delta$ (not visible in the figure). This observation resembles the behaviour which is well known from the standard EXAFS method (extended x-ray absorption fine structure) [25]. In reality, the photoelectron wave is scattered strongly from the potential discontinuities at the carbon ionic sites. Our model is capable of producing roughly this effect because the (average) bond length δ enters as the width of the potential well. In contrast to the qualitative form of the cross section, the amplitude of the oscillations of the experimental cross section is smaller than in our calculations. A softening of the oscillations may occur due to the wider energy profile of the density of the highest occupied state (than used in our model), and due to the screening of the electron–nucleus Coulomb interaction by the surrounding electrons as well as due to higher order scattering processes. Furthermore, we stress that the above explanation of the oscillations in SPI is just a crude, but useful physical picture that cannot reflect the effects of all the physical processes. For example, the mean field and the exchange effects, present in the form of the Hartree–Fock potentials are oscillatory and do not have sharp boundaries. In addition, the symmetry of a scattered wave is obviously decisive, as can be concluded from figure 2(b), in which case the SPI cross section from HOMO-1 has a different period of oscillation than in the case of HOMO.

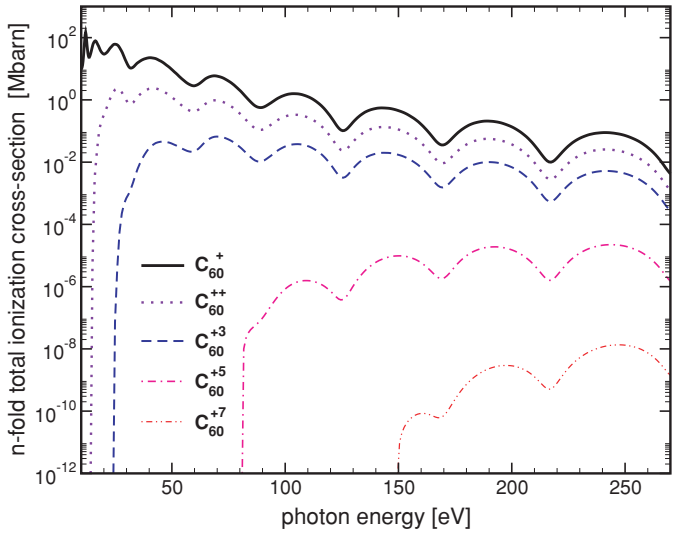

Figure 3. Different multiple-ionization cross sections of C_{60} following the absorption of a single photon. The charge state of the ionized fullerene is given by the numbers shown in the figure.

2.2. Effective electron–electron interaction

As is clear from equation (2) the calculations of the multiple ionization probabilities entail knowledge of the (e, 2e) scattering amplitude $T_{\mathrm{e}\,2\mathrm{e}}$, i.e. the probability that the scattering state with the wave vector $\mathbf{q}_i$ scatters from a valence electron orbital ϕ_{i+1} to result in two final scattering states characterized by the asymptotic momenta $\mathbf{k}_i$ and $\mathbf{q}_{i+1}$.

Within RPAE the transition amplitude $T_{\mathrm{e}\,2\mathrm{e}} = \langle \mathbf{k}_i \mathbf{q}_{i+1}|U|\phi_{i+1}\mathbf{q}_i\rangle$ is determined from the solution of the integral equation [1, 26]

$$\langle \mathbf{k}_i \mathbf{q}_{i+1}|U|\phi_{i+1}\mathbf{q}_i\rangle = \langle \mathbf{k}_i \mathbf{q}_{i+1}|u|\phi_{i+1}\mathbf{q}_i\rangle + \sum_{\epsilon_p \leqslant \mu < \epsilon_h} \left(\frac{\langle \varphi_p \mathbf{q}_{i+1}|U|\phi_{i+1}\varphi_h\rangle\langle \varphi_h \mathbf{k}_i|u|\mathbf{q}_i\varphi_p\rangle}{q_i^2/2 - (\epsilon_p - \epsilon_h - i\gamma)} - \frac{\langle \varphi_h \mathbf{q}_{i+1}|U|\phi_{i+1}\varphi_p\rangle\langle \varphi_p \mathbf{k}_i|u|\mathbf{q}_i\varphi_h\rangle}{q_i^2/2 + (\epsilon_p - \epsilon_h - i\gamma)} \right). \quad (4)$$

The first term on the rhs of this equation corresponds to the removal of an electron of the valence shell by virtue of the *naked* Coulomb interaction u with a scattering state electron. The second term originates from the change of the cluster potential due to interaction with other electrons of the system. The indices p and h in equation (4) label the particle and hole states above and below the Fermi level. The sum describes an admixture of the excited states to the initial state and implies a summation over unoccupied discrete levels and an integration over the continuum. In this way, the correlations are included as a modification to the perturbation due to the mobile electrons. The creation of the electron–hole pairs is mediated by the bare electron–electron interaction, $\langle mj|u|ki\rangle$. Due to the long-range character of u, the calculation of the numerous Coulomb matrix elements of these transitions is quite tedious and one has to develop efficient numerical methods to cope with this problem. Having calculated T_ω and $T_{\mathrm{e}\,2\mathrm{e}}$ we evaluate numerically the total (integrated) MPI cross sections. Technical details of the numerical procedure will be given elsewhere.

Examples of multiple photoionization cross sections from the highest occupied fullerene state are depicted in figure 3. The general behaviour of the multiple ionization cross sections is

determined by several factors. The oscillations in the cross sections are due to the oscillating nature of the single photoionization matrix element (cf figure 2), the origin of which we discussed above. The reason why these oscillations are still observable in multiple-ionization cross section is twofold: as shown in [1], $|T_{e,2e}(\omega)|^2$ is a smooth flat function of ω [1], i.e. $|T_{e,2e}(\omega)|^2$ acts as a smooth background (apart from the energy region near the ionization threshold). Secondly, in figure 3 we consider the ionization of one particular state, HOMO, of C_{60}. If more (or all) states are involved (as is the case in [16]), the oscillations will be smeared out. This is readily deduced from figure 2 which shows that the ionization cross sections from HOMO and HOMO-1 have different oscillation periods as a function of ω. Hence, in a state-non-resolved experiment the oscillations will be rather obscured. In addition, the averaging over the ionized electron quantum numbers, even when a single valence state is involved, makes the oscillations less pronounced, in particular for large n where numerous averaging procedures are involved.

Differences in the order of magnitudes for different n are governed mainly by the magnitude of the energy-dependent $|T_{e,2e}|^2$. Roughly speaking, for a certain energy, the n-fold ionization cross section scales as $|T_{e,2e}|^{2(n-1)}$. Hence, a smaller $|T_{e,2e}|^2$ leads to a substantial decrease of the cross section with increasing n. We note that $|T_{e,2e}|^2$ in the present context can be regarded as a measure of the strength of the two-particle interaction (in the presence of the surrounding inhomogeneous medium, accounted for at the level of RPAE). A negligible electron–electron interaction u and/or strong screening of u lead to diminishing multiple ionization cross sections (cf equations (1), (2), (4)).

3. Summary

In this work, we presented a model for the description of multiple ionization of the fullerene by a single photon. The n-fold ionization process is expressed as a single electron–photon and several electron–electron incoherent collisions, appropriately averaged over intermediate states. To account for dynamical screening effects of the electron–electron interaction in each collision event, we applied the random-phase approximation with exchange. The single and different multiple photoionization cross sections are calculated and analysed in the photon energy range [0, 250 eV]. The goal is to provide a reasonable estimate for the various multiple photoionization cross sections. In the authors' view, this goal is satisfactorily achieved. This statement derives from the level of agreement of $|T_\omega|^2$ with the experiments shown in figure 2 and from the previous finding that $|T_{e,2e}|^2$ is as well capable of describing (e, 2e) cross section data from C_{60} [1]. Unfortunately, the experimental results on MPI presently available are not state-resolved and hence cannot be directly compared to the calculations shown in figure 3 (taking into account all the 240 electrons and averaging over all possible initial states are presently not feasible due to limited computational resources). On the other hand, it is highly desirable to perform state-resolved measurements (in particular from HOMO) in order to rule out possible contributing channels (Auger processes, inference effects, etc). As for the general validity of the model we remark the following: $|T_\omega|^2$ and $|T_{e,2e}|^2$ are the critical quantities that enter the description of multiple ionization. Hence, the model is expected to perform well for a target with a large number of delocalized electrons for two reasons. The screening of the electron–electron interaction makes a single-scattering (Born-like) treatment of the electron–electron encounter more viable. Secondly, in each collision step the electron is scattered from a large number of scattering centres which motivates the assumption of a randomized phase of the scattering amplitudes with increasing number of scatterers.

Acknowledgment

We thank Nikolay Kabachnik for stimulating discussions and useful suggestions.

References

[1] Kidun O and Berakdar J 2001 *Phys. Rev. Lett.* **87** 263401
[2] Liechtenstein A I, Gunnarsson O, Knupfe M, Fink J and Armbruster J F 1996 *J. Phys.: Condens. Matter* **8** 4001
[3] Park H, Park J, Lim A K L, Anderson E H, Alivisatos A P and McEuen P L 2000 *Nature* **407** 57
[4] Yamachika R, Grobis M, Wachowiak A and Crommie M F 2004 *Science* **304** 281
[5] Rudolf P, Golden M S and Bruhwiller P A 1999 *J. Electron Spectrosc. Relat. Phenom.* **100** 409
[6] Campbell E and Rohmund F 2000 *Rep. Prog. Phys.* **63** 1061
[7] Forro L and Michaly L 2001 *Rep. Prog. Phys.* **64** 649
[8] Ajayan P M, Iijima S and Ichihashi T 1992 *Phys. Rev.* B **47** 6859
Yase K, Horiuchi S, Kyotani M, Yumura M, Uchida K, Ohshima S, Kuriki Y, Ikazaki F and Yamahira N 1996 *Thin Solid Films* **273** 222
Stöckli T, Bonard J-M, Stadelmann P A and Châtelain A 1997 *Z. Phys.* D **40** 425
[9] Berkowitz J 1999 *J. Chem. Phys.* **111** 1446
[10] Becker U, Gessner O and Rüdel A 2000 *J. Electron Spectrosc. Relat. Phenom.* **108** 189
[11] Rüdel A *et al* 2001 *Phys. Rev. Lett.* **89** 125503
[12] Matt S, Dünser B, Lezius M, Becker K, Stamatovic A, Scheier P and Märk T D 1996 *J. Chem. Phys.* **105** 1880
Foltin V, Foltin M, Matt S, Scheier P, Becker K, Deutsch H and Märk T D 1998 *Chem. Phys. Lett.* **289** 181
[13] Reinköster A, Werner U, Kabachnik N M and Lutz H O 2001 *Phys. Rev.* A **64** 23201
[14] Hathiramani D, Scheier P, Bräuning H, Trassl R, Salzborn E, Presnyakov L P, Narits A A and Uskov D B 2003 *Nucl. Instrum. Methods. Phys. Res.* B **212** 67
[15] Kou J, Mori T, Kumar S V K, Hariyama Y, Kubozono Y and Misuke K 2004 *J. Chem. Phys.* **120** 6005
[16] Reinköster A *et al* 2004 *J. Phys. B: At. Mol. Opt. Phys.* **37** 2135
[17] Russek A and Meli J 1970 *Physika* **46** 222
[18] Hansen K, Hoffmann K and Campbell E E B 2003 *J. Chem. Phys.* **119** 2522
[19] Kidun O, Fominykh N and Berakdar J 2002 *J. Phys. A: Math. Gen.* **35** 9413
[20] Babikov V 1971 *Method of the Phase Functions in Quantum Mechanics* (Moscow: Nauka)
[21] Calogero F 1967 *Variable Phase Approach to Potential Scattering* (New York: Academic)
[22] Brack M 1993 *Rev. Mod. Phys.* **65** 677
[23] Hasegawa S J, Miyamae T, Yakushi K, Inokuchi K, Seki K and Ueno N 1998 *Phys. Rev.* B **58** 4927
[24] Frank O and Rost J M 1997 *Chem. Phys. Lett.* **271** 367
[25] Teo B K and Joy D C (eds) 1981 *EXAFS Spectroscopy* (New York: Plenum)
[26] Amusia M Ya 1991 *Atomic Photoeffect* (New York: Academic)